

World Journal of *Gastroenterology*

World J Gastroenterol 2020 February 21; 26(7): 696-776



MINIREVIEWS

- 696 Proteomic insights on the metabolism in inflammatory bowel disease
Pisani LF, Moriggi M, Gelfi C, Vecchi M, Pastorelli L

ORIGINAL ARTICLE**Basic Study**

- 706 Liver stiffness and perfusion changes for hepatic sinusoidal obstruction syndrome in rabbit model
Shin J, Yoon H, Cha YJ, Han K, Lee MJ, Kim MJ, Shin HJ
- 717 Role of Tenascin-X in regulating TGF- β /Smad signaling pathway in pathogenesis of slow transit constipation
Zhang YC, Chen BX, Xie XY, Zhou Y, Qian Q, Jiang CQ

Retrospective Cohort Study

- 725 Pre-hepatectomy type IV collagen 7S predicts post-hepatectomy liver failure and recovery
Ishii M, Itano O, Shinoda M, Kitago M, Abe Y, Hibi T, Yagi H, Takeuchi A, Tsujikawa H, Abe T, Kitagawa Y
- 740 Biliary spontaneous dislodgement spiral stent for patients who underwent mechanical lithotripsy
Ye LS, Yuan XL, Wu CC, Liu W, Du J, Yao MH, Tan QH, Hu B

Retrospective Study

- 749 Modified Child-Pugh grade vs albumin-bilirubin grade for predicting prognosis of hepatocellular carcinoma patients after hepatectomy
Huang F, Gao J

Observational Study

- 759 Benefits of implementing a rapid access clinic in a high-volume inflammatory bowel disease center: Access, resource utilization and outcomes
Nene S, Gonczi L, Kurti Z, Morin I, Chavez K, Verdon C, Reinglas J, Kohen R, Bessissow T, Afif W, Wild G, Seidman E, Bitton A, Lakatos PL

CASE REPORT

- 770 Malignant glomus tumor of the intestinal ileum with multiorgan metastases: A case report and review of literature
Chen JH, Lin L, Liu KL, Su H, Wang LL, Ding PP, Zhou Q, Liu H, Wu J

ABOUT COVER

Associate Editor of *World Journal of Gastroenterology*, Peter L Lakatos, DSc, FEBG, MD, PhD, Full Professor, Division of Gastroenterology, Montreal General Hospital C7-200, McGill University Health Center, Quebec H3G1A4, Canada

AIMS AND SCOPE

The primary aim of *World Journal of Gastroenterology (WJG, World J Gastroenterol)* is to provide scholars and readers from various fields of gastroenterology and hepatology with a platform to publish high-quality basic and clinical research articles and communicate their research findings online.

WJG mainly publishes articles reporting research results and findings obtained in the field of gastroenterology and hepatology and covering a wide range of topics including gastroenterology, hepatology, gastrointestinal endoscopy, gastrointestinal surgery, gastrointestinal oncology, and pediatric gastroenterology.

INDEXING/ABSTRACTING

The *WJG* is now indexed in Current Contents®/Clinical Medicine, Science Citation Index Expanded (also known as SciSearch®), Journal Citation Reports®, Index Medicus, MEDLINE, PubMed, PubMed Central, and Scopus. The 2019 edition of Journal Citation Report® cites the 2018 impact factor for *WJG* as 3.411 (5-year impact factor: 3.579), ranking *WJG* as 35th among 84 journals in gastroenterology and hepatology (quartile in category Q2). CiteScore (2018): 3.43.

RESPONSIBLE EDITORS FOR THIS ISSUE

Responsible Electronic Editor: *Yu-Jie Ma*
 Proofing Production Department Director: *Xiang Li*

NAME OF JOURNAL

World Journal of Gastroenterology

ISSN

ISSN 1007-9327 (print) ISSN 2219-2840 (online)

LAUNCH DATE

October 1, 1995

FREQUENCY

Weekly

EDITORS-IN-CHIEF

Subrata Ghosh, Andrzej S Tarnawski

EDITORIAL BOARD MEMBERS

<http://www.wjgnet.com/1007-9327/editorialboard.htm>

EDITORIAL OFFICE

Ze-Mao Gong, Director

PUBLICATION DATE

February 21, 2020

COPYRIGHT

© 2020 Baishideng Publishing Group Inc

INSTRUCTIONS TO AUTHORS

<https://www.wjgnet.com/bpg/gerinfo/204>

GUIDELINES FOR ETHICS DOCUMENTS

<https://www.wjgnet.com/bpg/GerInfo/287>

GUIDELINES FOR NON-NATIVE SPEAKERS OF ENGLISH

<https://www.wjgnet.com/bpg/gerinfo/240>

PUBLICATION MISCONDUCT

<https://www.wjgnet.com/bpg/gerinfo/208>

ARTICLE PROCESSING CHARGE

<https://www.wjgnet.com/bpg/gerinfo/242>

STEPS FOR SUBMITTING MANUSCRIPTS

<https://www.wjgnet.com/bpg/GerInfo/239>

ONLINE SUBMISSION

<https://www.f6publishing.com>

Basic Study

Liver stiffness and perfusion changes for hepatic sinusoidal obstruction syndrome in rabbit model

Jaeseung Shin, Haesung Yoon, Yoon Jin Cha, Kyunghwa Han, Mi-Jung Lee, Myung-Joon Kim, Hyun Joo Shin

ORCID number: Jaeseung Shin (0000-0002-6755-4732); Haesung Yoon (0000-0003-0581-8656); Yoon Jin Cha (0000-0002-5967-4064); Kyunghwa Han (0000-0002-5687-7237); Mi-Jung Lee (0000-0003-3244-9171); Myung-Joon Kim (0000-0002-4608-0275); Hyun Joo Shin (0000-0002-7462-2609).

Author contributions: Shin HJ designed the research; Shin HJ, Shin J, Yoon H and Cha YJ performed the research; Shin HJ and Han K analyzed the data; Shin HJ and Shin J wrote the paper; Shin HJ, Lee M-J, Kim M-J, Yoon H, and Shin J revised and edited manuscript.

Supported by a Faculty Research Grant of Yonsei University College of Medicine for 2017, No. 6-2017-0090.

Institutional animal care and use committee statement: This study was approved by the Institution's Animal Care and Use Committee of Yonsei University Health System (IACUC approval no. 2017-0174).

Conflict-of-interest statement: Dr. Shin reports grants from Yonsei University College of Medicine, during the conduct of the study.

Data sharing statement: No additional data are available.

ARRIVE guidelines statement: The authors have read the ARRIVE guidelines, and the manuscript was prepared and revised according to the ARRIVE guidelines.

Jaeseung Shin, Haesung Yoon, Mi-Jung Lee, Myung-Joon Kim, Hyun Joo Shin, Department of Radiology, Severance Hospital, Research Institute of Radiological Science, Yonsei University College of Medicine, Seoul 03722, South Korea

Yoon Jin Cha, Department of Pathology, Gangnam Severance Hospital, Yonsei University College of Medicine, Seoul 06273, South Korea

Kyunghwa Han, Department of Radiology, Severance Hospital, Research Institute of Radiological Science, Center for Clinical Imaging Data Science, Seoul 03722, South Korea

Corresponding author: Hyun Joo Shin, MD, PhD, Clinical Assistant Professor, Department of Radiology, Severance Hospital, Research Institute of Radiological Science, Yonsei University College of Medicine, 50-1 Yonsei-ro, Seodaemun-gu, Seoul 03722, South Korea.
lamer-22@yuhs.ac

Abstract

BACKGROUND

Hepatic sinusoidal obstruction syndrome (SOS) is caused by damage to hepatic sinusoidal endothelial cells that results in fibrous obliteration of intrahepatic venules and necrosis of hepatocytes. Currently the diagnosis is primarily based on nonspecific clinical features and invasive liver biopsy. Therefore, noninvasive imaging methods are required for the early diagnosis and severity assessment of hepatic SOS.

AIM

To determine the effectiveness of supersonic shear wave imaging (SSI) and dual energy computed tomography (DECT) for diagnosing hepatic SOS using a rabbit model.

METHODS

Among nine New Zealand white rabbits (3-4 kg, male), three in control group ingested normal saline for 20 d and six in the SOS group ingested 6-thioguanine (5 mg/kg/d) for 20 d. Liver stiffness was measured using SSI on days 0, 3, 10, and 20. On the same days, liver perfusion was evaluated from virtual monochromatic images of 55 keV and iodine map using DECT. Morphologic changes in the liver were assessed using CT. Final pathology scores were compared between the two groups. Liver stiffness and perfusion parameters were compared according to the groups, days, and pathology scores.

RESULTS

Final pathology scores were significantly higher in the SOS than the control

Open-Access: This article is an open-access article that was selected by an in-house editor and fully peer-reviewed by external reviewers. It is distributed in accordance with the Creative Commons Attribution NonCommercial (CC BY-NC 4.0) license, which permits others to distribute, remix, adapt, build upon this work non-commercially, and license their derivative works on different terms, provided the original work is properly cited and the use is non-commercial. See: <http://creativecommons.org/licenses/by-nc/4.0/>

Manuscript source: Unsolicited manuscript

Received: October 29, 2019

Peer-review started: October 29, 2019

First decision: December 23, 2019

Revised: January 8, 2020

Accepted: January 19, 2020

Article in press: January 19, 2020

Published online: February 21, 2020

P-Reviewer: Colecchia A

S-Editor: Dou Y

L-Editor: A

E-Editor: Ma YJ



group (median 22 *vs* 2, $P = 0.024$). No gross morphologic changes were seen in livers. Liver stiffness, Hounsfield Unit values, and iodine concentrations were higher in the SOS compared to the control group on days 10 and 20 (all, $P \leq 0.007$). Compared to day 0, liver stiffness and perfusion parameters were higher on day 20 in the SOS group (all, $P \leq 0.001$). Correlation coefficients for liver stiffness ($r = 0.635$), Hounsfield Unit values ($r = 0.587$), and iodine concentration ($r = 0.611$) with final pathology scores were positive without significance (all, $P > 0.05$).

CONCLUSION

Liver stiffness and perfusion parameters were significantly increased in the livers of a rabbit SOS model. SSI and DECT might aid in early diagnosis of hepatic SOS.

Key words: Hepatic sinusoidal obstruction syndrome; Elasticity imaging techniques; Iodine; Computed tomography; Liver; Animals

©The Author(s) 2020. Published by Baishideng Publishing Group Inc. All rights reserved.

Core tip: Noninvasive imaging methods are required for the early diagnosis and severity assessment of hepatic sinusoidal obstruction syndrome (SOS). This study showed that liver stiffness on supersonic shear wave imaging was significantly elevated as hepatic SOS progressed in rabbit model. In addition, as hepatic SOS progressed, perfusion parameters measured on dual energy computed tomography were significantly elevated. We suggested that quantitative imaging with supersonic shear wave imaging and dual energy computed tomography could aid in the early diagnosis of hepatic SOS.

Citation: Shin J, Yoon H, Cha YJ, Han K, Lee MJ, Kim MJ, Shin HJ. Liver stiffness and perfusion changes for hepatic sinusoidal obstruction syndrome in rabbit model. *World J Gastroenterol* 2020; 26(7): 706-716

URL: <https://www.wjgnet.com/1007-9327/full/v26/i7/706.htm>

DOI: <https://dx.doi.org/10.3748/wjg.v26.i7.706>

INTRODUCTION

Hepatic sinusoidal obstruction syndrome (SOS) is a well-known serious complication of hematopoietic stem cell transplantation (HSCT) and is associated with drugs including oxaliplatin-based chemotherapy^[1-4]. Hepatic SOS, also known as hepatic veno-occlusive disease, is caused by damage to hepatic sinusoidal endothelial cells that results in fibrous obliteration of intrahepatic venules and necrosis of centrilobular hepatocytes^[3,5]. In pediatric patients, SOS is the most common cause of death after graft-versus-host reaction and infection in patients with HSCT with nonspecific symptoms of painful hepatomegaly, fluid retention, and hyperbilirubinemia^[3,6]. Liver biopsy is the gold standard for the diagnosis of hepatic SOS, but is limited because of its invasiveness, interobserver variation, and sampling error. Even though conventional computed tomography (CT) or ultrasonography (US) have demonstrated that gross changes in hepatic SOS, such as heterogeneous hypoattenuation and patchy parenchymal enhancement with narrowing of hepatic veins, those imaging findings are nonspecific and present after disease progression while diagnosing hepatic SOS in clinical setting^[7]. Therefore, new noninvasive imaging biomarker for early diagnosis and severity assessment of hepatic SOS are required as alternatives to liver biopsy and conventional imaging modalities^[8].

US elastography is a noninvasive tool for evaluating liver stiffness. In addition to transient elastography (TE) validated for assessment of liver fibrosis^[9,10], shear wave elastography (SWE) uses ultrasound waves to quantify the tissue-specific propagation speed of shear waves for guidance of grayscale US images^[11,12]. SWE gives more reliable results than TE^[13]. Supersonic shear wave imaging (SSI) is a recently introduced SWE technique characterized by ultrafast image acquisition using multiple push beams and a color map with a wide range. SSI enables real-time analysis with color display, a large field of view and multiple regions of interest, for advantages over acoustic radiation force impulse (ARFI). Although a few studies reported elevated liver stiffness using TE and ARFI in a rat or human SOS^[14-18] and patients

undergoing HSCT^[19,20], no study has evaluated liver stiffness in hepatic SOS using SSI.

Dual energy CT (DECT) uses photon spectra generated by two distinctive tube voltages to obtain additional information about tissue composition based on spectral properties^[21]. With material-specific information, virtual monochromatic images (VMIs) and concentration map images of materials such as iodine and calcium can be generated by DECT for quantitative diagnosis of liver steatosis and fibrosis^[22-24]. In hepatic SOS, toxic injury to sinusoidal endothelial cells might cause loss of autoregulation and reduction of blood flow in the sinusoids^[1]. We postulated that these events could result in different iodine concentrations in livers with SOS, but little has been published on DECT imaging in hepatic SOS. Therefore, the purpose of this study was to know liver stiffness and perfusion changes using SSI and DECT for diagnosis of hepatic SOS using a rabbit model.

MATERIALS AND METHODS

Animal model

This study was approved by our institution's Animal Experimental Committee and performed according to local animal care guidelines. Nine male New Zealand white rabbits weighting 3-4 kg were used. Three rabbits ingested normal saline *via* a 1 cc syringe for 20 d and were the control group. Six rabbits ingested 6-thioguanine (6-TG, 5 mg/kg/d, four days in a week) for 20 d according to a previous study^[25] and were the SOS group. Rabbits received standard diets during the experiments. Rabbit conditions were monitored by radiologists and a veterinarian.

Laboratory studies

On days 0, 3, 10, and 20 during medication, laboratory and imaging examinations were performed under sedation. Sedation was accomplished by intramuscular injection of xylazine hydrochloride (1 mg/kg, Rompun; Bayer Korea, Seoul, South Korea) and intravenous injection of alfaxalone (3 mg/kg, Alfaxan®; Careside, Gyeonggi-do, South Korea) with the help of a veterinarian before starting examinations.

Laboratory tests were performed with samples from ear veins. Tests were for serum aspartate aminotransferase (AST), alanine aminotransferase (ALT), total bilirubin (Tbil), and direct bilirubin (Dbil) levels.

Imaging studies

For imaging studies, SWE and DECT were performed on days 0, 3, 10, and 20. Rabbits were in a supine position on the scan table, with forelegs up and tightened with bandages. The upper abdomen was shaved for contact with the US probe. For SWE, SSI (Aixplorer, SuperSonic Imagine, Aix-en-Provence, France; software version of 9.2) was used with a 10-2 MHz linear transducer. An experienced pediatric radiologist performed examinations. Liver stiffness was measured for the liver parenchyma at an epigastric area because in rabbits, the liver left lobe was large and had fewer artifacts from bowel loops than other lobes. Color maps were made for the liver parenchyma avoiding hepatic vessels and bile ducts. A round region of interest (ROI) with diameter 2-4 mm and depth of about 1.5 cm was put on color maps when maps appeared homogeneous during regular free breathing without intubation. Mean value for liver stiffness within the ROI was automatically recorded in kPa units based on Young's modulus. Measurements were repeated seven times as in a previous study^[26] and mean values were recorded (Figure 1A). All processes were repeated twice and two representative values were used for each rabbit.

CT was performed using DECT with fast kVp switching (80/140 kVp) on a single-source dual-energy 64-channel multidetector CT scanner (GE Discovery CT750 HD scanner, GE Healthcare, Milwaukee, Wisconsin, United States) on the same days. Contrast agent iobitridol (Xenetics 300, Guerbet, Roissy, France) at 2 cc/kg was manually injected into an auricular vein, using the same institutional protocol as for neonates. Scanning parameters were: Helical mode, rapid kVp switching between 80 and 140 kVp, tube current 260 mA, detector collimation 64 mm × 0.625 mm, acquisition mode in axial plane, slice thickness 2.5 mm, pitch 1.375:1, soft convolution kernel, and CT dose index volume 6.48 mGy. Single-phase portal venous phase was acquired at fixed time delay 40 s following contrast material injection according to the institutional CT scan protocol for neonates. Livers were scanned in the craniocaudal direction.

Morphologic liver changes during the study period were assessed using CT. A pediatric radiologist assessed the presence of liver parenchymal as heterogeneous patchy enhancement, gallbladder (GB) wall edema, narrowed or invisible hepatic

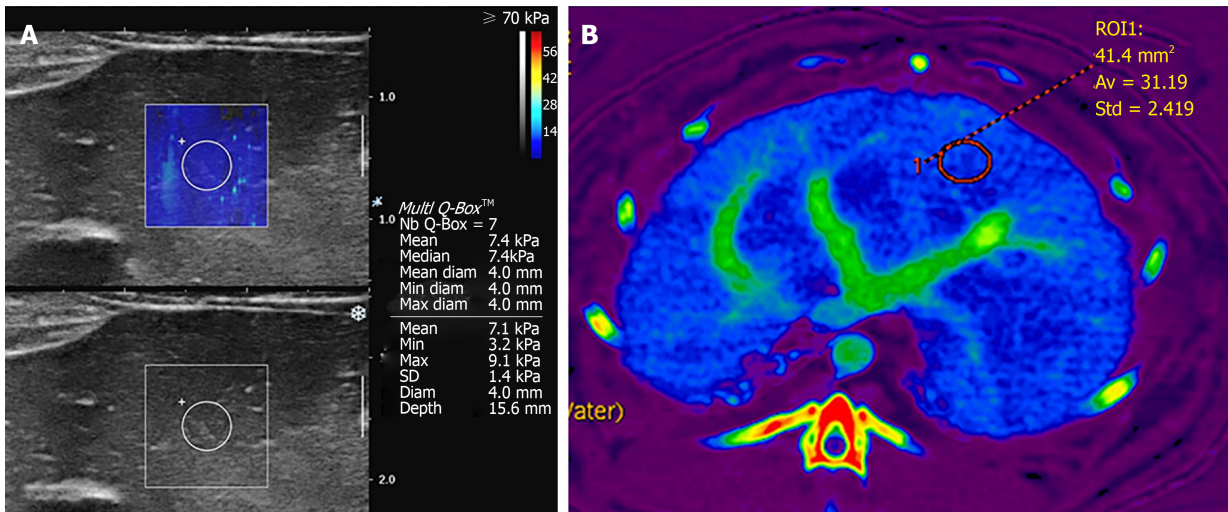


Figure 1 Representative images from supersonic shear wave imaging and dual energy computed tomography of rabbits in a sinusoidal obstruction syndrome group on day 20. A: Mean liver stiffness value for livers in the sinusoidal obstruction syndrome group was 7.4 kPa; B: Iodine concentration in livers of the sinusoidal obstruction syndrome group was 31.19 mg/mL.

veins, hepatomegaly showing inferior liver margin below the right kidney, or presence of ascites using DECT images according to previous studies^[7,27,28].

For quantitative assessments, filtered back projection images without iterative reconstruction were used for reconstruction and analysis. VMIs at 55 keV were used for analysis because 70 or 80 kVp images were routinely used for neonate abdominal CT in our hospital. Material density iodine maps were reconstructed. Round ROIs were drawn in liver parenchyma avoiding hepatic vessels using an AW server (GE Healthcare, Milwaukee, Wisconsin, United States; software version 2.0). ROIs were positioned in the same place in the liver parenchyma on VMI 55 keV image and iodine map (Figure 1B). Mean CT attenuations in Hounsfield units (HUs) and iodine concentrations (mg/mL) within ROIs were recorded. ROIs were drawn three times over liver parenchyma and three values were acquired for each parameter.

Radiation dose using mean effective dose by multiplying dose-length product with k (conversion factor, 0.049 used for pediatric patients younger than one year old) of all rabbits were assessed.

Pathologic scoring of hepatic SOS

On day 21, rabbits were sacrificed and hepatic specimens were obtained. Specimens were fixed in 10% phosphate-buffered formalin (pH 7.1) for 24 h and put in 70% ethanol. After obtaining paraffin blocks, hematoxylin and eosin, Masson's trichrome, and Verhoeff-Van Gieson staining was performed. Final pathology scores for SOS were assessed by an experienced board-certificated pathologist according to a scoring system used previously^[25]. Scores were assessed as the sum of each subscore in three categories: sinusoidal, central vein, and necro-inflammatory damage. For evaluating sinusoidal damage, sinusoidal dilatation, or congestion were evaluated using subscores from 0 to 3. For evaluation of central vein damage, fraying of endothelial cells and sludge in central veins were assessed. For the evaluation of necro-inflammatory damage, apoptotic bodies, inflammatory cell infiltrates, steatosis, and necrosis were scored separately. All scores were evaluated for 10 areas in lower power fields; the possible range of scores 0 to 240. The pathologist was blind to the final diagnosis of the rabbits.

Statistical analysis

Statistical analysis was done with SAS (version 9.4, SAS Institute Inc., Cary, NC, United States). Final pathology scores between control and SOS groups were compared using Mann-Whitney U tests. Differences in changing pattern of laboratory results and quantitative imaging parameters including liver stiffness on SSI, HU values on VMI 55 keV images, and iodine concentration (mg/mL) on iodine maps were assessed using linear mixed models. Values were compared between groups for each day and compared between days 0 and 20 for each group in post hoc analysis. Spearman's correlation tests were used to determine correlations between results measured on day 20 and final pathology scores. *P* values less than 0.05 were considered statistically significant.

RESULTS

During the study period, three of six rabbits in the SOS group died unexpectedly on days 10, 11, and 17. Results for these rabbits until the day of unexpected death were used as much as possible. Pathology results were obtained on the day of death for these rabbits, except the rabbit that died on day 17. The remaining three rabbits in the SOS group all had examinations on days 0, 3, 10, and 20 and pathology results on day 21. Therefore, days 0 and 3 had results from all six rabbits, while day 10 had results from 5 rabbits, and day 20 had results from 3 rabbits in the SOS group. The three rabbits in the control group were alive through day 20.

Final pathology scores were significantly higher in the SOS group ($n = 5$, range 20-42, median 22) than the control group ($n = 3$, range 2-11, median 2) ($P = 0.024$). According to the categories, the sum of scores for sinusoidal damage was 121 in the SOS group and 15 in the control group. For central vein damage, the score was 3 for the SOS group and 0 for the control group. For necro-inflammatory damage, the score was 9 for the SOS group and 0 for the control group. Liver parenchymal patchy heterogeneous enhancement, GB wall edema, narrowed or invisible hepatic veins, hepatomegaly, or ascites were not presented in CT images for both SOS and control groups during the study period. The mean effective dose of DECT was 7.9 ± 1.6 mSv for all rabbits.

Using linear mixed models, we saw significant differences in changing patterns of liver stiffness, HU values in VMI 55 keV, and iodine concentration between two groups (all, $P < 0.001$) (Figure 2). Laboratory results showed no significant differences between the two groups in patterns over 20 d. Post hoc analyses of laboratory and imaging studies are in Table 1 and 2. Compared to controls, on day 20, AST, ALT, and D.bil values were significantly higher in the SOS group ($P = 0.004$, 0.008, 0.013, respectively) (Table 1). Liver stiffness values were significantly higher in the SOS group on day 10 (9.48 kPa vs 4.02 kPa, $P < 0.001$) and day 20 (7.71 kPa vs 4.67 kPa, $P = 0.007$) compared to the control group (Table 2). HU values for VMI 55 keV were significantly higher in the SOS group on day 3 (167.68 HU vs 147.18 HU, $P = 0.045$), day 10 (185.42 HU vs 129.05 HU, $P < 0.001$) and day 20 (179.81 HU vs 148.95 HU, $P = 0.006$). Iodine concentrations were significantly higher in the SOS group on day 3 (26.74 mg/mL vs 20.72 mg/mL, $P = 0.022$), day 10 (31.86 mg/mL vs 19.16 mg/mL, $P < 0.001$), and day 20 (35.14 mg/mL vs 23.85 mg/mL, $P < 0.001$).

When comparing laboratory results, AST, ALT, and Dbil values were significantly higher on day 20 than on day 0 in the SOS group ($P = 0.001$, 0.001, and 0.004, respectively), while there were no significant differences between days 0 and 20 in the control group (Table 3). In quantitative imaging studies (Table 4), liver stiffness values were significantly higher on day 20 than on day 0 in the SOS group (7.71 kPa vs 3.89 kPa, $P < 0.001$), but there was no significant difference of stiffness between day 0 and day 20 in the control group (4.67 kPa vs 4.35 kPa, $P = 0.752$) (Table 4). HU values for VMI 55 keV were significantly higher on day 20 in the SOS group (179.81 HU vs 158.77 HU, $P = 0.001$), with no differences in the control group (147.95 HU vs 153.18 HU, $P = 0.510$). Iodine concentrations were also significantly higher on day 20 in the SOS group (35.14 mg/mL vs 24.2 mg/mL, $P < 0.001$), with no differences in the control group (23.85 mg/mL vs 24.8 mg/mL, $P = 0.539$).

In assessing correlations among final pathology scores and laboratory results (Table 5), correlation coefficients were 0.323 for AST, 0.491 for ALT, 0.156 for Tbil, and 0.261 for Dbil, without statistical significance ($P > 0.05$). In imaging studies, correlation coefficients were 0.635 for liver stiffness, 0.587 for VMI 55 keV, and 0.611 for iodine concentration, even without statistical significance ($P > 0.05$).

DISCUSSION

In our animal study, hepatic SOS was induced in a rabbit model by orally administered 6-TG. As described by Oancea *et al*^[25], orally administered 6-TG causes hepatic SOS in a dose-dependent manner in a murine model and our findings confirmed early and acute sinusoidal injury in rabbit model by pathology. Our pathology results showed early and acute changes in the SOS group, which was different from the control group. Because rabbits in the SOS group did not show morphologic changes on CT images, these results confirmed the early disease stages of our rabbit model. In this model, non-invasive SSI and DECT examinations had promising results for diagnosing hepatic SOS. Our study was meaningful because changes in quantitative imaging studies with SSI and DECT occurred earlier than morphologic changes in conventional CT.

Our SSI results indicated that hepatic SOS led to elevated liver stiffness. Significant

Table 1 Comparison of laboratory results between control and sinusoidal obstruction syndrome groups

Results	Days	Control group	SOS group	Differences	P value
AST (IU/L)	0	32.67 (-55.57, 120.9)	20.5 (-41.89, 82.89)	12.17 (-95.9, 120.23)	0.818
	3	24.67 (-63.57, 112.9)	23 (-39.39, 85.39)	1.67 (-106.4, 109.73)	0.975
	10	20.67 (-67.57, 108.9)	26.4 (-42.5, 95.3)	-5.73 (-117.68, 106.22)	0.917
	20	26.33 (-61.9, 114.57)	221.34 (130.35, 312.33)	-195.01 (-321.75, -68.26)	0.004 ^b
ALT (IU/L)	0	38 (3.97, 72.03)	33.17 (9.11, 57.23)	4.83 (-36.84, 46.51)	0.813
	3	44.67 (10.64, 78.69)	41.83 (17.77, 65.89)	2.83 (-38.84, 44.51)	0.890
	10	33.67 (-0.36, 67.69)	25.41 (-1.18, 51.99)	8.26 (-34.92, 51.44)	0.697
	20	40.67 (6.64, 74.69)	109.35 (74.12, 144.58)	-68.69 (-117.67, -19.71)	0.008 ^b
Tbil (mg/dL)	0	0.27 (-0.18, 0.72)	0.42 (0.1, 0.73)	-0.15 (-0.7, 0.4)	0.579
	3	0.63 (0.18, 1.08)	0.52 (0.2, 0.83)	0.12 (-0.43, 0.67)	0.666
	10	0.9 (0.45, 1.35)	1.18 (0.82, 1.53)	-0.28 (-0.85, 0.29)	0.328
	20	0.53 (0.08, 0.98)	0.96 (0.49, 1.43)	-0.43 (-1.07, 0.22)	0.186
Dbil (mg/dL)	0	0.1 (-0.08, 0.28)	0.12 (-0.01, 0.25)	-0.02 (-0.24, 0.21)	0.879
	3	0.13 (-0.05, 0.32)	0.17 (0.04, 0.3)	-0.03 (-0.26, 0.19)	0.760
	10	0.17 (-0.02, 0.35)	0.26 (0.12, 0.4)	-0.09 (-0.32, 0.14)	0.411
	20	0.13 (-0.05, 0.32)	0.47 (0.28, 0.65)	-0.33 (-0.59, -0.08)	0.013 ^a

Values are estimated mean and 95% confidence interval.

^aP < 0.05.

^bP < 0.01. SOS: Sinusoidal obstruction syndrome; AST: Serum aspartate aminotransferase; ALT: Alanine aminotransferase; Tbil: Total bilirubin; Dbil: Direct bilirubin.

stiffness changes measured by SSI were observed starting on day 10, with no obvious morphologic change even with contrast enhanced CT throughout the test days. To the best of our knowledge, this is the first study to investigate the effectiveness of SSI for assessing hepatic SOS. SSI has benefits such as a large area to measure, ultrafast imaging, and low failure rate compared with TE or ARFI^[29]. Previous studies with TE or ARFI reported an increased liver stiffness in a rat model^[14] and in pediatric or adult patients following HSCT^[15-18,30]. A study demonstrated that SWE detects earlier changes than color Doppler study in SOS^[20]. Increased liver stiffness could be from hepatic venous congestion in the SOS model, although liver inflammation and cholestasis could also affect increased liver stiffness^[31]. Our study confirmed that SSI could be a method for monitoring disease progression or treatment response to SOS. The SSI values were highest on day 10 and decreased on day 20. Attention is required to interpret decreased SSI value on day 20 because of the relatively small number of animals at day 20. Further clinical research is required to prove the potential utility of SSI in the detection and follow up of hepatic SOS.

Previous studies with conventional CT reported nonspecific morphologic changes such as hepatomegaly, ascites, heterogeneous patchy parenchymal enhancement, narrowed hepatic veins, and GB wall edema for diagnosis of hepatic SOS; these might lack sensitive detection for early changes in hepatic SOS^[28,32]. Our study demonstrated that quantitative DECT showed increased HU values on VMI 55 keV and increased iodine concentrations in material density maps in the liver parenchyma before gross morphologic changes occurred. These quantitative values also showed increasing trends throughout the study period, which may be promising for follow-up of the severity of hepatic SOS. Low-keV images using VMI could enhance iodine effects^[33]. This method could aid in the detection of changing patterns of iodine accumulation in the liver parenchyma in hepatic SOS using low-keV images and iodine maps.

Increased HU values and iodine concentrations in our study might be from iodine congestion due to endothelial injury of sinusoids and small intrahepatic venules. A previous study found that on pathology, hepatic SOS showed blood stagnation in dilated sinusoids^[32]. However, heterogeneous hypoattenuation and patchy liver enhancement were observed in a small number of SOS patients following neoadjuvant chemotherapy or pyrrolizidine alkaloid ingestion^[7,27,34,35]. These heterogeneous hypoattenuations might be related to delayed blood inflow and decreased flow velocity from damaged sinusoids filled with cell debris, red cells, and extracellular matrix^[34,35]. Different patterns of enhancement in hepatic SOS could be from different stages and etiologies of SOS according to the studies. Delayed blood flow and decreased flow velocity from hepatic SOS could represent an advanced stage and this could be different from our study. Our study found iodine accumulation in

Table 2 Comparison of quantitative imaging results between control and sinusoidal obstruction syndrome groups

Parameters	Days	Control group	SOS group	Differences	P value
Liver stiffness (kPa)	0	4.35 (2.82, 5.88)	3.89 (2.81, 4.97)	0.46 (-1.41, 2.33)	0.623
	3	5.68 (4.16, 7.21)	6.38 (5.3, 7.45)	-0.69 (-2.56, 1.18)	0.458
	10	4.02 (2.49, 5.54)	9.48 (8.29, 10.66)	-5.46 (-7.39, -3.53)	< 0.001 ^b
	20	4.67 (3.14, 6.19)	7.71 (6.17, 9.25)	-3.04 (-5.21, -0.87)	0.007 ^b
VMI 55 keV (HU)	0	153.18 (137.07, 169.29)	158.77 (147.38, 170.16)	-5.59 (-25.33, 14.14)	0.550
	3	147.18 (131.07, 163.29)	167.68 (155.92, 179.44)	-20.5 (-40.44, -0.55)	0.045 ^a
	10	129.05 (112.94, 145.16)	185.42 (173.62, 197.22)	-56.37 (-76.34, -36.4)	< 0.001 ^b
	20	148.95 (132.83, 165.06)	179.81 (166.5, 193.11)	-30.86 (-51.69, -10.03)	0.006 ^b
Iodine concentration (mg/mL)	0	24.8 (20.76, 28.84)	24.2 (21.34, 27.05)	0.61 (-4.34, 5.55)	0.794
	3	20.72 (16.69, 24.76)	26.73 (23.79, 29.67)	-6.01 (-11, -1.02)	0.022 ^a
	10	19.16 (15.12, 23.19)	31.86 (28.91, 34.8)	-12.7 (-17.7, -7.7)	< 0.001 ^b
	20	23.85 (19.81, 27.88)	35.14 (31.84, 38.44)	-11.29 (-16.49, -6.1)	< 0.001 ^b

Values are estimated mean and 95% confidence interval.

^aP < 0.05.

^bP < 0.01. SOS: Sinusoidal obstruction syndrome; VMI: Virtual monochromatic image; HU: Hounsfield unit.

the liver parenchyma in the acute stage of the SOS from blood stagnation. Endothelial injuries and edema of sinusoids could occur in early stage SOS, while hepatic necrosis and deposition of collagen, fibrous tissues could occur in disease progression^[7]. Therefore, different stages of SOS might have different enhancement patterns. A previous study suggested that the etiology of SOS could cause different enhancement patterns because tumor-related factors also alter liver perfusion and steatosis could affect liver attenuation after receiving chemotherapy^[34]. Direct quantification of iodine in the liver parenchyma with DECT may be a possible objective method for overcoming the inherent ambiguous nature of attenuation in livers with SOS using conventional CT^[24,36]. Further studies for assessing DECT results according to stage and etiology of SOS in patients are needed.

This study has several limitations. First, the small number of animals and unexpected death in SOS group in this experimental study was the main reason for the lack of statistical significance in the correlation between final pathology scores and laboratory results or imaging parameters, even though correlation coefficients were about 0.6 for quantitative imaging results. Second, we did not assess hepatic arterial resistance index or flow direction of the portal vein using Doppler US in rabbits. Third, rabbits were assessed until day 20 and advanced disease stages with apparent morphologic changes were not evaluated. However, because this study demonstrated the potential effectiveness of SSI and DECT for hepatic SOS, further large studies with patients and animal models are needed.

In conclusion, changes of quantitative parameters with SSI and DECT could aid the diagnosis of hepatic SOS before morphologic changes were apparent in the liver of a rabbit model. Liver stiffness on SSI, HU values on VMI with low keV, and iodine concentrations on DECT were significantly increased in livers according to SOS progression.

Table 3 Comparison of laboratory results between days 0 and 20

Results	Groups	Day 0	Day 20	Difference	P value
AST (IU/L)	Control	32.67 (-55.57, 120.9)	26.33 (-61.9, 114.57)	6.33 (-118.48, 131.15)	0.916
	SOS	20.5 (-41.89, 82.89)	221.34 (130.35, 312.33)	-200.84 (-310.9, -90.78)	0.001 ^b
ALT (IU/L)	Control	38 (3.97, 72.03)	40.67 (6.64, 74.69)	-2.67 (-51.54, 46.21)	0.910
	SOS	33.17 (9.11, 57.23)	109.35 (74.12, 144.58)	-76.19 (-119.14, -33.24)	0.001 ^b
Tbil (mg/dL)	Control	0.27 (-0.18, 0.72)	0.53 (0.08, 0.98)	-0.27 (-0.9, 0.37)	0.387
	SOS	0.42 (0.1, 0.73)	0.96 (0.49, 1.43)	-0.54 (-1.1, 0.02)	0.057
Dbil (mg/dL)	Control	0.1 (-0.08, 0.28)	0.13 (-0.05, 0.32)	-0.03 (-0.29, 0.22)	0.792
	SOS	0.12 (-0.01, 0.25)	0.47 (0.28, 0.65)	-0.35 (-0.57, -0.13)	0.004 ^b

Values are presented as estimated mean and 95% confidence interval.

^b*P* < 0.01. SOS: sinusoidal obstruction syndrome; AST: Serum aspartate aminotransferase; ALT: Alanine aminotransferase; Tbil: Total bilirubin; Dbil: Direct bilirubin.

Table 4 Comparison of quantitative imaging results between day 0 and 20

Parameters	Groups	Day 0	Day 20	Difference	P value
Liver stiffness (kPa)	Control	4.35 (2.82, 5.88)	4.67 (3.14, 6.19)	-0.32 (-2.32, 1.69)	0.752
	SOS	3.89 (2.81, 4.97)	7.71 (6.17, 9.25)	-3.82 (-5.61, -2.02)	< 0.001 ^b
VMI 55 keV (HU)	Control	153.18 (137.07, 169.29)	148.95 (132.83, 165.06)	4.23 (-8.48, 16.95)	0.510
	SOS	158.77 (147.38, 170.16)	179.81 (166.5, 193.11)	-21.04 (-32.7, -9.37)	0.001 ^b
Iodine concentration (mg/mL)	Control	24.8 (20.76, 28.84)	23.85 (19.81, 27.88)	0.95 (-2.12, 4.03)	0.539
	SOS	24.2 (21.34, 27.05)	35.14 (31.84, 38.44)	-10.94 (-13.77, -8.12)	< 0.001 ^b

Values are presented as estimated mean and 95% confidence interval.

^b*P* < 0.01. SOS: Sinusoidal obstruction syndrome; VMI: Virtual monochromatic image; HU: Hounsfield unit.

Table 5 Assessment of correlation between final pathologic scores and laboratory results and quantitative imaging parameters

Results	<i>r</i> (95%CI)	P value
AST (IU/L)	0.323 (-0.511, 0.83)	0.453
ALT (IU/L)	0.491 (-0.358, 0.881)	0.230
Tbil (mg/dL)	0.156 (-0.623, 0.771)	0.726
Dbil (mg/dL)	0.261 (-0.557, 0.809)	0.551
Liver stiffness (kPa)	0.635 (-0.171, 0.919)	0.094
VMI 55 keV (HU)	0.587 (-0.241, 0.906)	0.133
Iodine concentration (mg/mL)	0.611 (-0.207, 0.913)	0.112

AST: Serum aspartate aminotransferase; ALT: Alanine aminotransferase; Tbil: Total bilirubin; Dbil: Direct bilirubin; VMI: Virtual monochromatic image; HU: Hounsfield unit; CI: Confidence interval.

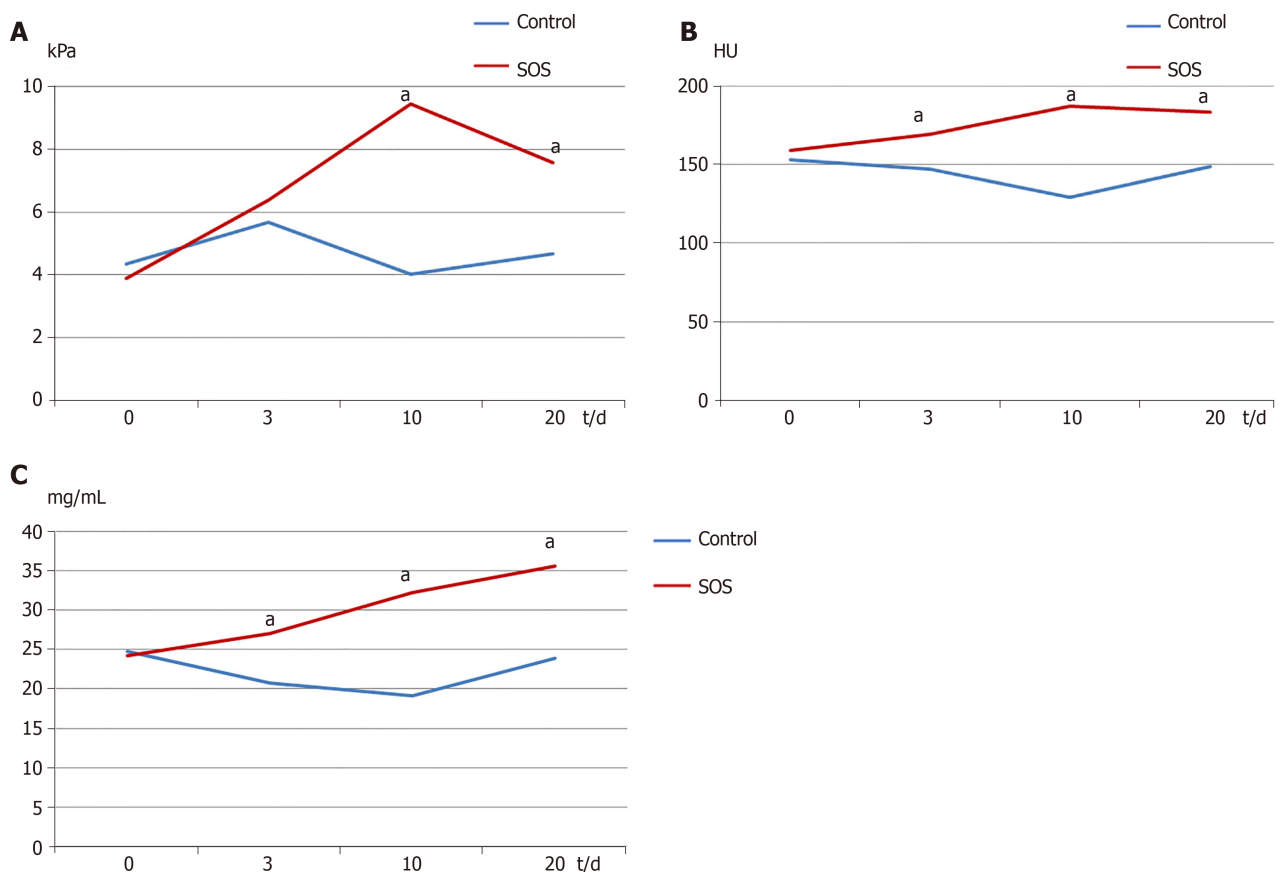


Figure 2 Changing patterns of imaging results. A: Liver stiffness on supersonic shear wave imaging; B: Hounsfield unit values on virtual monochromatic image of 55 keV; C: Iodine concentration on iodine map of dual energy computed tomography on days 0, 3, 10, and 20 in control (blue) and sinusoidal obstruction syndrome (SOS) (red) groups. All three quantitative values showed significant differences in changing pattern between control and SOS groups for all days ($P < 0.001$). ^aShows significantly different results between control and SOS groups for each day.

ARTICLE HIGHLIGHTS

Research background

Hepatic sinusoidal obstruction syndrome (SOS) is a well-known serious complication of hematopoietic stem cell transplantation and is associated with chemotherapy. Noninvasive imaging methods are required for the early diagnosis and severity assessment of hepatic SOS.

Research motivation

In pediatric patients, SOS is the most common cause of death in patients with hematopoietic stem cell transplantation with nonspecific symptoms. Currently the diagnosis is primarily based on nonspecific clinical features and invasive liver biopsy. Therefore, noninvasive imaging methods are required for the early diagnosis and severity assessment of hepatic SOS. Supersonic shear wave imaging (SSI) is a recently introduced US elastography technique and is a noninvasive tool for evaluating liver stiffness. Dual energy computed tomography (DECT) could quantify tissue composition or iodine concentration. We postulated that these imaging studies could quantify liver stiffness and perfusion changes in hepatic SOS.

Research objectives

The purpose of the study was to determine the effectiveness of SSI and DECT for diagnosing hepatic SOS using a rabbit model.

Research methods

Among nine New Zealand white rabbits, three were in control group and six with 6-thioguanine ingestion were in SOS group. Liver stiffness was measured using SSI and liver perfusion was evaluated from virtual monochromatic images of 55 keV and iodine map using DECT on days 0, 3, 10, and 20. Liver stiffness and perfusion parameters were compared according to the groups, days, and pathology scores.

Research results

Compared to the control group, final pathology scores were significantly higher in the SOS group, while there were no gross morphologic changes using conventional imaging. Liver stiffness, Hounsfield Unit values, and iodine concentrations were higher in the SOS compared to

the control group as disease progression.

Research conclusions

This study showed that liver stiffness on SSI and perfusion parameters on DECT were significantly increased according to SOS progression in a rabbit model. We suggested that quantitative imaging with SSI and DECT could aid in the early diagnosis of hepatic SOS.

Research perspectives

SSI and DECT could be the noninvasive imaging studies for early diagnosis and severity assessment of hepatic SOS. Because this study demonstrated the potential effectiveness of SSI and DECT for hepatic SOS, further large studies with patients are needed.

ACKNOWLEDGEMENTS

Authors thank to In Sook Yang, Department of Laboratory Animal Resources, Avison BioMedical Research Center, Yonsei University College of Medicine, for her help in animal preparation.

REFERENCES

- 1 **Rubbia-Brandt L.** Sinusoidal obstruction syndrome. *Clin Liver Dis* 2010; **14**: 651-668 [PMID: 21055688 DOI: 10.1016/j.cld.2010.07.009]
- 2 **Rubbia-Brandt L,** Audard V, Sartoretti P, Roth AD, Brezault C, Le Charpentier M, Dousset B, Morel P, Soubrane O, Chaussade S, Mentha G, Terris B. Severe hepatic sinusoidal obstruction associated with oxaliplatin-based chemotherapy in patients with metastatic colorectal cancer. *Ann Oncol* 2004; **15**: 460-466 [PMID: 14998849]
- 3 **Hasegawa S,** Horibe K, Kawabe T, Kato K, Kojima S, Matsuyama T, Hirabayashi N. Veno-occlusive disease of the liver after allogeneic bone marrow transplantation in children with hematologic malignancies: incidence, onset time and risk factors. *Bone Marrow Transplant* 1998; **22**: 1191-1197 [PMID: 9894723 DOI: 10.1038/sj.bmt.1701506]
- 4 **Mohty M,** Malard F, Abecassis M, Aerts E, Alaskar AS, Aljurf M, Arat M, Bader P, Baron F, Bazarbachi A, Blaise D, Ciceri F, Corbacioglu S, Dalle JH, Duarte RF, Fukuda T, Huynh A, Masszi T, Michallet M, Nagler A, NiChonghaile M, Pagluica T, Peters C, Petersen FB, Richardson PG, Ruutu T, Savani BN, Wallhult E, Yakoub-Agha I, Carreras E. Sinusoidal obstruction syndrome/veno-occlusive disease: current situation and perspectives-a position statement from the European Society for Blood and Marrow Transplantation (EBMT). *Bone Marrow Transplant* 2015; **50**: 781-789 [PMID: 25798682 DOI: 10.1038/bmt.2015.52]
- 5 **DeLeve LD,** McCuskey RS, Wang X, Hu L, McCuskey MK, Epstein RB, Kanel GC. Characterization of a reproducible rat model of hepatic veno-occlusive disease. *Hepatology* 1999; **29**: 1779-1791 [PMID: 10347121 DOI: 10.1002/hep.510290615]
- 6 **McCarville MB,** Hoffer FA, Howard SC, Goloubeva O, Kauffman WM. Hepatic veno-occlusive disease in children undergoing bone-marrow transplantation: usefulness of sonographic findings. *Pediatr Radiol* 2001; **31**: 102-105 [PMID: 11214676 DOI: 10.1007/s002470000373]
- 7 **Yang S,** Wu J, Lei S. CT Features of Hepatic Veno-occlusive Disease: A Meta-analysis. *Acad Radiol* 2018; **25**: 328-337 [PMID: 29191686 DOI: 10.1016/j.acra.2017.10.012]
- 8 **Ravaioli F,** Colecchia A, Alemanni LV, Vestito A, Dajti E, Marasco G, Sessa M, Pession A, Bonifazi F, Festi D. Role of imaging techniques in liver veno-occlusive disease diagnosis: recent advances and literature review. *Expert Rev Gastroenterol Hepatol* 2019; **13**: 463-484 [PMID: 30895833 DOI: 10.1080/17474124.2019.1588111]
- 9 **Nobili V,** Vizzutti F, Arena U, Abraldes JG, Marra F, Pietrobattista A, Fruhwirth R, Marcellini M, Pinzani M. Accuracy and reproducibility of transient elastography for the diagnosis of fibrosis in pediatric nonalcoholic steatohepatitis. *Hepatology* 2008; **48**: 442-448 [PMID: 18563842 DOI: 10.1002/hep.22376]
- 10 **Friedrich-Rust M,** Ong MF, Martens S, Sarrazin C, Bojunga J, Zeuzem S, Herrmann E. Performance of transient elastography for the staging of liver fibrosis: a meta-analysis. *Gastroenterology* 2008; **134**: 960-974 [PMID: 18395077 DOI: 10.1053/j.gastro.2008.01.034]
- 11 **Chen S,** Liao B, Zhong Z, Zheng Y, Liu B, Shan Q, Xie X, Zhou L. Supersonic shearwave elastography in the assessment of liver fibrosis for postoperative patients with biliary atresia. *Sci Rep* 2016; **6**: 31057 [PMID: 27511435 DOI: 10.1038/srep31057]
- 12 **Tutar O,** Beşer ÖF, Adaletli I, Tunc N, Gulcu D, Kantarci F, Mihmanli I, Cokugras FC, Kutlu T, Ozbay G, Erkan T. Shear wave elastography in the evaluation of liver fibrosis in children. *J Pediatr Gastroenterol Nutr* 2014; **58**: 750-755 [PMID: 24552673 DOI: 10.1097/MPG.0000000000000329]
- 13 **Woo H,** Lee JY, Yoon JH, Kim W, Cho B, Choi BI. Comparison of the Reliability of Acoustic Radiation Force Impulse Imaging and Supersonic Shear Imaging in Measurement of Liver Stiffness. *Radiology* 2015; **277**: 881-886 [PMID: 26147680 DOI: 10.1148/radiol.2015141975]
- 14 **Park SH,** Lee SS, Sung JY, Na K, Kim HJ, Kim SY, Park BJ, Byun JH. Noninvasive assessment of hepatic sinusoidal obstructive syndrome using acoustic radiation force impulse elastography imaging: A proof-of-concept study in rat models. *Eur Radiol* 2018; **28**: 2096-2106 [PMID: 29218616 DOI: 10.1007/s00330-017-5179-z]
- 15 **Auberger J,** Graziadei I, Clausen J, Vogel W, Nachbaur D. Non-invasive transient elastography for the prediction of liver toxicity following hematopoietic SCT. *Bone Marrow Transplant* 2013; **48**: 159-160 [PMID: 22705804 DOI: 10.1038/bmt.2012.113]
- 16 **Colecchia A,** Marasco G, Ravaioli F, Kleinschmidt K, Masetti R, Prete A, Pession A, Festi D. Usefulness of liver stiffness measurement in predicting hepatic veno-occlusive disease development in patients who undergo HSCT. *Bone Marrow Transplant* 2017; **52**: 494-497 [PMID: 27941774 DOI: 10.1038/bmt.2016.320]

- 17 **Karlas T**, Weber J, Nehring C, Kronenberger R, Tenckhoff H, Mössner J, Niederwieser D, Tröltzsch M, Lange T, Keim V. Value of liver elastography and abdominal ultrasound for detection of complications of allogeneic hemopoietic SCT. *Bone Marrow Transplant* 2014; **49**: 806-811 [PMID: [24710567](#) DOI: [10.1038/bmt.2014.61](#)]
- 18 **Zama D**, Bossù G, Ravaioli F, Masetti R, Prete A, Festi D, Pession A. Longitudinal evaluation of liver stiffness in three pediatric patients with veno-occlusive disease. *Pediatr Transplant* 2019; **23**: e13456 [PMID: [31081161](#) DOI: [10.1111/ptr.13456](#)]
- 19 **Colecchia A**, Ravaioli F, Sessa M, Alemanni VL, Dajti E, Marasco G, Vestito A, Zagari RM, Barbato F, Arpinati M, Cavo M, Festi D, Bonifazi F. Liver Stiffness Measurement Allows Early Diagnosis of Veno-Occlusive Disease/Sinusoidal Obstruction Syndrome in Adult Patients Who Undergo Hematopoietic Stem Cell Transplantation: Results from a Monocentric Prospective Study. *Biol Blood Marrow Transplant* 2019; **25**: 995-1003 [PMID: [30660772](#) DOI: [10.1016/j.bbmt.2019.01.019](#)]
- 20 **Reddivalla N**, Robinson AL, Reid KJ, Radhi MA, Dalal J, Opfer EK, Chan SS. Using liver elastography to diagnose sinusoidal obstruction syndrome in pediatric patients undergoing hematopoietic stem cell transplant. *Bone Marrow Transplant* 2018 [PMID: [29335626](#) DOI: [10.1038/s41409-017-0064-6](#)]
- 21 **Zhu X**, McCullough WP, Mecca P, Servaes S, Darge K. Dual-energy compared to single-energy CT in pediatric imaging: a phantom study for DECT clinical guidance. *Pediatr Radiol* 2016; **46**: 1671-1679 [PMID: [27518078](#) DOI: [10.1007/s00247-016-3668-x](#)]
- 22 **Heye T**, Nelson RC, Ho LM, Marin D, Boll DT. Dual-energy CT applications in the abdomen. *AJR Am J Roentgenol* 2012; **199**: S64-S70 [PMID: [23097169](#) DOI: [10.2214/AJR.12.9196](#)]
- 23 **Hyodo T**, Yada N, Hori M, Maenishi O, Lamb P, Sasaki K, Onoda M, Kudo M, Mochizuki T, Murakami T. Multimaterial Decomposition Algorithm for the Quantification of Liver Fat Content by Using Fast-Kilovolt-Peak Switching Dual-Energy CT: Clinical Evaluation. *Radiology* 2017; **283**: 108-118 [PMID: [28212047](#) DOI: [10.1148/radiol.2017160130](#)]
- 24 **Patino M**, Prochowski A, Agrawal MD, Simeone FJ, Gupta R, Hahn PF, Sahani DV. Material Separation Using Dual-Energy CT: Current and Emerging Applications. *Radiographics* 2016; **36**: 1087-1105 [PMID: [27399237](#) DOI: [10.1148/rg.2016150220](#)]
- 25 **Oancea I**, Png CW, Das I, Lourie R, Winkler IG, Eri R, Subramaniam N, Jinnah HA, McWhinney BC, Levesque JP, McGuckin MA, Duley JA, Florin TH. A novel mouse model of veno-occlusive disease provides strategies to prevent thioguanine-induced hepatic toxicity. *Gut* 2013; **62**: 594-605 [PMID: [22773547](#) DOI: [10.1136/gutjnl-2012-302274](#)]
- 26 **Shin HJ**, Kim MJ, Kim HY, Roh YH, Lee MJ. Optimal Acquisition Number for Hepatic Shear Wave Velocity Measurements in Children. *PLoS One* 2016; **11**: e0168758 [PMID: [28002480](#) DOI: [10.1371/journal.pone.0168758](#)]
- 27 **Kan X**, Ye J, Rong X, Lu Z, Li X, Wang Y, Yang L, Xu K, Song Y, Hou X. Diagnostic performance of Contrast-enhanced CT in Pyrrolizidine Alkaloids-induced Hepatic Sinusoidal Obstructive Syndrome. *Sci Rep* 2016; **6**: 37998 [PMID: [27897243](#) DOI: [10.1038/srep37998](#)]
- 28 **Erturk SM**, Mortelé KJ, Binkert CA, Glickman JN, Oliva MR, Ros PR, Silverman SG. CT features of hepatic venoocclusive disease and hepatic graft-versus-host disease in patients after hematopoietic stem cell transplantation. *AJR Am J Roentgenol* 2006; **186**: 1497-1501 [PMID: [16714636](#) DOI: [10.2214/ajr.05.0539](#)]
- 29 **Shin HJ**, Kim MJ, Kim HY, Roh YH, Lee MJ. Comparison of shear wave velocities on ultrasound elastography between different machines, transducers, and acquisition depths: a phantom study. *Eur Radiol* 2016; **26**: 3361-3367 [PMID: [26815368](#) DOI: [10.1007/s00330-016-4212-y](#)]
- 30 **Lazzari L**, Marra P, Greco R, Giglio F, Clerici D, Venturini E, Paesano P, Albanese S, Serio F, Ciceri F, Peccatori J. Ultrasound elastography techniques for diagnosis and follow-up of hepatic veno-occlusive disease. *Bone Marrow Transplant* 2019; **54**: 1145-1147 [PMID: [30679827](#) DOI: [10.1038/s41409-019-0432-5](#)]
- 31 **Dietrich CF**, Trenker C, Fontanilla T, Görg C, Hausmann A, Klein S, Lassau N, Miquel R, Schreiber-Dietrich D, Dong Y. New Ultrasound Techniques Challenge the Diagnosis of Sinusoidal Obstruction Syndrome. *Ultrasound Med Biol* 2018; **44**: 2171-2182 [PMID: [30076031](#) DOI: [10.1016/j.ultrasmedbio.2018.06.002](#)]
- 32 **Cayet S**, Pasco J, Dujardin F, Besson M, Orain I, De Muret A, Miquelstorena-Standley E, Thierry J, Genet T, Le Bayon AG. Diagnostic performance of contrast-enhanced CT-scan in sinusoidal obstruction syndrome induced by chemotherapy of colorectal liver metastases: Radio-pathological correlation. *Eur J Radiol* 2017; **94**: 180-190 [PMID: [28712693](#) DOI: [10.1016/j.ejrad.2017.06.025](#)]
- 33 **Siegel MJ**, Ramirez-Giraldo JC. Dual-Energy CT in Children: Imaging Algorithms and Clinical Applications. *Radiology* 2019; **291**: 286-297 [PMID: [30912717](#) DOI: [10.1148/radiol.2019182289](#)]
- 34 **Bethke A**, Kühne K, Platzek I, Stroszczyński C. Neoadjuvant treatment of colorectal liver metastases is associated with altered contrast enhancement on computed tomography. *Cancer Imaging* 2011; **11**: 91-99 [PMID: [21771709](#) DOI: [10.1102/1470-7330.2011.0015](#)]
- 35 **Han NY**, Park BJ, Kim MJ, Sung DJ, Cho SB. Hepatic Parenchymal Heterogeneity on Contrast-enhanced CT Scans Following Oxaliplatin-based Chemotherapy: Natural History and Association with Clinical Evidence of Sinusoidal Obstruction Syndrome. *Radiology* 2015; **276**: 766-774 [PMID: [25822471](#) DOI: [10.1148/radiol.2015141749](#)]
- 36 **Marin D**, Boll DT, Mileto A, Nelson RC. State of the art: dual-energy CT of the abdomen. *Radiology* 2014; **271**: 327-342 [PMID: [24761954](#) DOI: [10.1148/radiol.14131480](#)]



Published By Baishideng Publishing Group Inc
7041 Koll Center Parkway, Suite 160, Pleasanton, CA 94566, USA
Telephone: +1-925-3991568
E-mail: bpgoffice@wjgnet.com
Help Desk: <http://www.f6publishing.com/helpdesk>
<http://www.wjgnet.com>

